Electrochimica Acta 114 (2013) 533–542

Contents lists available at ScienceDirect

Electrochimica Acta

journal homepage: www.elsevier.com/locate/electacta

Chemically modified graphene and nitrogen-doped graphene: Electrochemical characterisation and sensing applications

Krishna P. Prathish[a], Madalina M. Barsan[a], Dongsheng Geng[b], Xueliang Sun[b], Christopher M.A. Brett[a,*]

[a] Departamento de Química, Faculdade de Ciências e Tecnologia, Universidade de Coimbra, 3004-535 Coimbra, Portugal
[b] Department of Mechanical and Materials Engineering, The University of Western Ontario, London, ON, Canada N6A 5B9

ARTICLE INFO

Article history:
Received 1 September 2013
Received in revised form 10 October 2013
Accepted 11 October 2013
Available online xxx

Keywords:
Nitrogen doped graphene
Functionalised graphene
Composite materials
Polymer-modified electrodes
Enzyme cofactors

ABSTRACT

Functionalised graphene (G) and nitrogen doped graphene (NG) nanomaterials are excellent candidates for electrocatalytic sensing of biomolecules and for developing biosensors, due to their unique physicochemical and electronic properties. Electrochemical characterisation and comparison of basic or acidic functionalised G and NG has been carried out, as well as of composite materials based on NG with the conducting polymer poly(3,4-ethylenedioxythiophene) (PEDOT) and the redox polymer poly(neutral red) by cyclic voltammetry and electrochemical impedance spectroscopy. Electroactive areas and heterogeneous electron transfer constant, of the GCE modified with the graphene derivatives have been evaluated, in order to choose the best material for electrode modification. The NG modified GCE enabled excellent electrocatalytic regeneration of the enzyme cofactors β-nicotinamide adenine dinucleotide (NADH) and flavin adenine dinucleotide (FAD), underlining the applicability of NG for the development of new sensitive biosensors.

© 2013 Elsevier Ltd. All rights reserved.

1. Introduction

Direct electron transfer at bioelectronic interfaces is one of the key questions in developing biosensor technology, as well as significantly enriching biofuel cell development. The redox centres of most enzymes are embedded deep inside the enzyme, and facilitating efficient electron transfer to the electrode surface is a challenging task [1]. Several methods have been adopted in order to establish electrical communication between redox enzymes and electrodes, first by using carbon nanotube, metal nanoparticle or graphene modified electrodes as sensor substrates, and secondly by employing electron transfer mediators, tethering of redox relay units to enzymes, or reconstitution of the apo-enzyme on relay cofactor units associated with electrodes [1–6].

During the past few decades, carbon-based nanomaterials have been widely used in electrochemical sensors due to their excellent catalytic activity, superior conductivity, large surface area, ease of functionalisation and biocompatibility [7]. They include the conventional carbon black, graphite, carbon nanotubes, fullerenes, up to the latest innovation of 2D graphene nano sheets. Graphene has been an attractive material due to its excellent conductivity, feasibility for microfabrication, high surface area, mechanical strength, optical transparency and biocompatibility [8,9]. Graphene consists of sp^2 hybridised carbon atoms, in which the valence and the conduction band overlap at the Brillouin zone, making pure graphene a zero band gap semiconductor, which limits its application potential due to its chemical inertness [10,11].

Doping with heteroatoms such as boron or nitrogen is an excellent method to open up the band gap and provide pathways for efficient electron transfer processes, transforming graphene into a p- or n-type semiconductor, a promising material in electrochemical biosensing, in supercapacitors and in fuel cells [10–13]. Up until now, such heteroatom doping was found to be successful in carbon nanotubes [14,15]. The introduction of a band gap can generate remarkable properties in graphene, analogous to CNTs. The one-dimensional nature of CNTs makes it difficult to controllably assemble CNTs whereas the 2D nature of graphene makes it suitable for microfabrication. Another important advantage of graphene over CNTs is the absence of metallic impurities [16,17]. Theoretical studies on adsorbate or substitutional B, N or O doped graphene has proved that substitutional doping, when heteroatoms are incorporated into the honeycomb structure of graphene, is more effective than the adsorption of heteroatoms on the graphene surface [12]. Substitution with an electron-rich heteroatom such as N, P etc. will result in n-type characteristics whereas an electron deficient atom like B induces a p-type characteristics, both of which cause an increase in free charge carriers in the graphene framework, thereby enhancing conductivity. Hence tuning the band gap

* Corresponding author. Tel.: +351 239854470; fax: +351 239827703.
E-mail address: cbrett@ci.uc.pt (C.M.A. Brett).

0013-4686/$ – see front matter © 2013 Elsevier Ltd. All rights reserved.
http://dx.doi.org/10.1016/j.electacta.2013.10.080

by chemical doping enhances the charge carrier concentration [18] and leads to promising applications in semiconductor electronics such as field effect transistors [11], and as electrocatalyst in the oxygen-reduction reaction (ORR) in fuel cells and in sensors [19].

The present study focuses on the electrochemical characterisation of functionalised graphene (G) and N-doped graphene (NG) and their application in sensing and biosensing. The N-doping of graphene has been done by thermal annealing in the presence of ammonia and the nitrogen atom in the graphene framework can exist in "graphitic", pyridinic or pyrrolic forms, each of which can provide different characteristics to the graphene framework [19,20]. Pure and N-graphene were compared with their derivatives, which were acidic (HNO_3) or basic (KOH) functionalised G and NG [21,22]. Composite materials based on NG with the conducting polymer poly(3,4-ethylenedioxythiphene) (PEDOT) and the redox polymer poly(neutral red) (PNR) were also synthesised. To fully exploit the electrochemical properties of the different types of graphene and composite graphene, electrochemical characterisation was performed at graphene modified GCE by cyclic voltammetry (CV) and electrochemical impedance spectroscopy (EIS) without and with the standard electroactive species $K_4[Fe(CN)_6]$. To our knowledge, the electrochemistry of NG and its acidic and/or basic functionalised analogues and polymer composites with NG have not yet been thoroughly investigated, so that the present work brings a deeper knowledge and comparison of their electrochemical characteristics. The graphene material with the best electrochemical properties has been applied to the detection of important cofactors present in oxidase and dehydrogenase based enzymes, i.e. β-nicotinamide adenine dinucleotide (NADH) and flavin adenine dinucleotide (FAD), the regeneration of which is the crucial step during an enzyme reaction, and thence for biosensor performance.

2. Experimental

2.1. Reagents and buffer electrolyte solutions

All reagents were of analytical grade and were used without further purification. Graphene and N-doped graphene, prepared by thermal reduction of graphite oxide, were characterised in [23]. Graphite, chitosan (low molecular weight), 2,3-dihydrothieno[3,4-*b*]-1,4-dioxin (EDOT), glutaraldehyde, neutral red (NR) 65% dye content, nicotinamide dinucleotide, monobasic and dibasic potassium phosphate, sodium chloride and sodium poly(styrene sulfonate) (NaPSS) were from Sigma-Aldrich, Germany. Flavine adenine dinucleotide, potassium hexacyanoferrate(II) trihydrate, potassium chloride, monobasic sodium phosphate and were obtained from Fluka, Switzerland.

For electrochemical experiments, the supporting electrolytes were 0.1 M KCl or sodium phosphate buffer saline (NaPBS) (0.1 M phosphate buffer + 0.05 M NaCl, pH = 7.0). Polymerisation of NR was carried out in 0.025 M potassium phosphate buffer solution plus 0.1 M KNO_3 (pH 5.5) containing 1 mM NR and of EDOT in 0.1 M NaPSS containing 10 mM EDOT.

Millipore Milli-Q nanopure water (resistivity $\geq$18 MΩ cm) was used for the preparation of all solutions. All experiments were performed at room temperature (25 ± 1 °C).

2.2. Instrumentation

Electrochemical experiments were performed in a three electrode cell, containing a glassy carbon electrode (GCE) (area 0.237 cm^2) as working electrode, a Pt wire counter electrode and an Ag/AgCl (3.0 M KCl) reference electrode, using a potentiostat/galvanostat μ-Autolab system (Metrohm-Autolab, Netherlands).

Electrochemical impedance spectroscopy (EIS) experiments were carried out with a potentiostat/galvanostat/ZRA, (Gamry Instruments, Reference 600). An rms perturbation of 10 mV was applied over the frequency range 100 kHz to 0.1 Hz, with 10 frequency values per frequency decade.

The pH measurements were carried out with a CRISON 2001 micro pH-meter (Crison Instruments SA, Barcelona, Spain) at room temperature.

2.3. Functionalisation of graphene and N-graphene and preparation of modified electrodes

Graphene (G) and nitrogen doped G (NG) were used as received or treated either in 3 M HNO_3 or in 7 M KOH. For the acidic treatment, the graphene or graphite (Gr) powder was stirred during for 12 h, while for the treatment with base, stirring was during 4 h followed by another 20 h static soaking in ambient conditions. The functionalised particles were then washed and filtered with Milli-Q water until the solution become neutral. The material obtained was dried at ≈60 °C overnight. In this way we obtained HNO_3_G/NG/Gr and KOH_G/NG. Due to the fact that HNO_3 treatment of NG was detrimental, the dispersion not being homogeneous and the modified electrodes being very unstable, this material was not used further in this study.

Both functionalised and un-functionalised G and NG were dispersed in 1% (w/v) chitosan dissolved in 1% (v/v) acetic acid, to form a 0.1% dispersion. The solution was sonicated for 1 h and vortexed before 20 μl was drop cast on the GCE. The modified electrodes were left overnight to dry.

2.4. Preparation of PEDOT/NG and PNR/NG modified electrodes

Four types of composite of NG with conducting polymer PEDOT and the redox polymer PNR were prepared: NG/PEDOT, PEDOT/NG, NG/PNR and PNR/NG. In the first and third case, the GCE was first drop cast with NG followed by electropolymerisation of EDOT and NR, whereas in the second and fourth, electropolymerisation of EDOT/NR was done prior to the drop casting of NG.

Both monomers were electropolymerised by cyclic voltammetry in the solutions described in Section 2.1, at a scan rate of 50 mV s^{-1}, between −1.0 and +1.0 V vs. Ag/AgCl for 15 cycles, for NR and from −0.6 V to 1.2 V vs. Ag/AgCl for 20 cycles for EDOT.

3. Results and discussion

Elemental, structural and surface morphological characterisation of the graphene and N-doped graphene has been carried out previously [23], one of the main conclusions being that more defects are present on nitrogen-doped graphene.

The electrochemical characterisation of the G and NG modified electrodes and their functionalised derivatives was undertaken in order to evaluate potential windows, electroactive areas and apparent heterogeneous rate constant (k_0). EIS measurements allowed confirmation of results obtained by CV and, furthermore, to explore surface and bulk characteristics of the graphene-modified electrodes. This permitted choosing the best graphene materials for sensing/biosensing application. Their electrocatalytic properties for the determination of the very important enzyme cofactors NADH and FAD was evaluated.

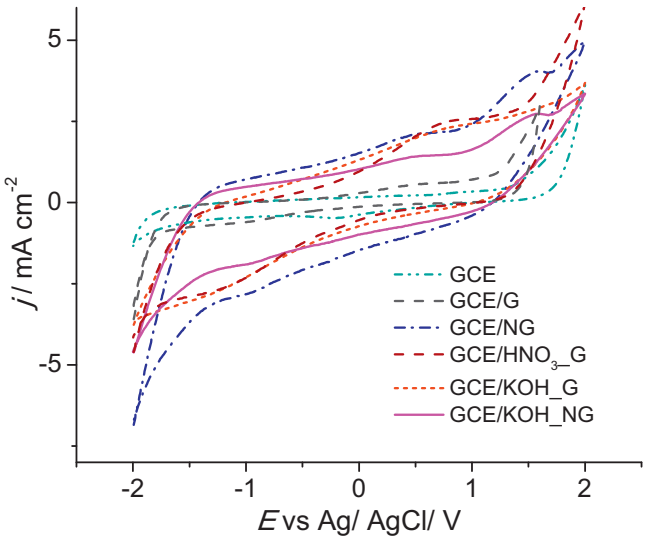

Fig. 1. Cyclic voltammograms recorded at GCE, and GCE modified with G and NG derivatives in 0.1 M NaPBS pH 7.0; $\upsilon = 100\,mV\,s^{-1}$.

3.1. Potential windows and electroactive areas of G and NG and derivatives

The potential windows of G, NG, HNO_3_G and KOH_G/NG modified GCE were tested in neutral, acidic (down to pH 2.0) and basic media (up to pH 10.0). CVs recorded in 0.1 M NaPBS pH 7.0 are displayed in Fig. 1. The modified electrodes exhibited wide potential windows in all tested media, from ≈−1.8 up to 1.8 V vs. Ag/AgCl. Untreated graphene increased the capacitive current compared to bare GCE by a factor of 1.8, while the NG, HNO_3_G and KOH_G/NG increased it substantially, by a factor of ≈10, underlying the importance in doping or functionalising graphene in order to improve its electrochemical properties. The sp^2 hybridised structure of graphene contributes to the high capacitive nature of these materials which are of prime importance in developing supercapacitors and fuel cells [12].

Cyclic voltammograms of G, NG, HNO_3_G and KOH_G/NG modified GCE were recorded in the presence of the standard electroactive redox probe $K_4[Fe(CN)_6]$ in 0.1 M KCl at scan rates ranging from 10 to 200 mV s^{-1} (see Fig. 2a_1 and b_1, as examples for NG and HNO_3_G). Well-defined anodic and cathodic peaks were recorded for all the modified electrodes. Anodic and cathodic peak currents were plotted against square root of scan rate, as shown in Fig. 2a_2 and b_2, the linearity of the plots ($R^2 = 0.998$) confirming diffusion-controlled electron transfer in all cases. Slight shifts in peak potential were observed with increasing scan rate indicating some kinetic limitations.

The electroactive areas (A_{ele}) of the modified electrodes tested were determined using the Randles-Sevčik equation [24]:

$$I_p = 2.69 \times 10^5 A D^{1/2} n^{3/2} C \upsilon^{1/2} \quad (1)$$

where I_p is the anodic peak current (A), A is the electroactive area (cm^2), D is the diffusion coefficient of $[Fe(CN)_6]^{4-}$ in solution, $6.1 \times 10^{-6}\,cm^2\,s^{-1}$ calculated according to [25], n is the number of electrons transferred in the redox reaction, υ is the potential scan rate ($V\,s^{-1}$), and C is the $[Fe(CN)_6]^{4-}$ concentration in bulk solution ($mol\,cm^{-3}$). The results are given in Table 1. It can be seen that the electroactive area of GCE/G is comparable to that of GCE, because without functionalisation or doping, graphene is highly hydrophobic, so that diffusion of electrolyte is hindered. The HNO_3_G and KOH_G/NG modified GCE increased the electroactive area by a factor of almost 3, 280% × A_{geom} for HNO_3_G and KOH_G and 290% × A_{geom} for KOH_NG. For comparison, HNO_3-treated graphite (HNO_3_Gr) was also deposited on GCE and the electroactive area was determined to be 190% × A_{geo}, much lower than functionalised G and NG, good evidence that graphene does not form graphite sheets during the preparation of the modified electrodes. The NG-modified electrode had the highest electroactive area, of 430% × A_{geom}, indicating clearly the advantageous effect of electron-rich nitrogen atom incorporation.

Apparent heterogeneous rate constants (k_0) were calculated from the difference in anodic and cathodic peak potentials in CV and the values are also displayed in Table 1. HNO_3_G and KOH_NG gave the highest values, of $6.9 \times 10^{-4}\,cm\,s^{-1}$, the lowest being that of bare GCE and GCE/G, of 2.41 and $2.80 \times 10^{-4}\,cm\,s^{-1}$, respectively. The heterogeneous rate constants are influenced by various factors such as the microstructure of the electrode material, particularly edge plane defects on the surface, surface roughness, and the presence of surface functional groups [26]. Functionalisation of G or NG by acid treatment will result in the formation of carboxyl, hydroxyl, carbonyl, and nitro functional groups at the defect sites, which improves the material's hydrophilicity and conductivity, while KOH treatment allows the formation of a 3D network of small pore size [22], both leading to an increase of the heterogeneous rate constant and electroactive area.

3.2. Fabrication and evaluation of NG-based composites with PEDOT and PNR

Conducting and redox polymers can be used together with nanoscale materials in order to improve their conductivity and/or to increase their electrocatalytic activity. NG was selected to test the influence of PEDOT and PNR on the overall electrochemical properties of the composites, since GCE/NG exhibited the highest electroactive area. As mentioned in Section 2.4, four types of composites based on NG with the conducting polymer PEDOT and the redox polymer PNR were prepared, namely NG/PEDOT, PEDOT/NG, NG/PNR and PNR/NG.

As observed, there are differences in the CV profile recorded during polymerisation of EDOT on bare GCE and on GCE/NG (see Fig. 3 a_1 and a_2). On top of GCE, a large amount of polymer is formed, indicated by the increase in the capacitance from 1.8 to 23.6 mF cm^{-2}, similar to that reported in [27], but only a small amount of polymer was deposited on GCE/NG, the capacitance increasing from 5.0 mF cm^{-2}, due to the capacitive properties of NG itself, only to 7.8 mF cm^{-2}. This clearly suggests that more PEDOT is formed on bare GCE. Probably, polymer formed inside the porous NG structure may obstruct the entry of EDOT monomer molecules, so that polymer formation is more difficult.

Differences in the CV profile during NR polymerisation are also noticeable, regarding the main reduction wave and the second pair of peaks at more positive potentials around 0.25 V vs. Ag/AgCl. While at bare GCE (Fig. 3b_1) the main reduction peak shifts towards negative potentials by 300 mV during polymerisation, at GCE/NG it remains constant (Fig. 3b_2), so that the redox polymer peaks are closer than at bare GCE ($\Delta E_p = 0.15$ V compared to $\Delta E_p = 0.40$ V at GCE). The fact that the second pair of peaks at 0.25 V is significantly more visible at NG substrates, it is also advantageous. The same polymerisation profile obtained at GCE/NG was obtained at carbon composite electrodes [28] and GCE/CNT [29,30] modified GCE, being therefore correlated with the nanoscale particle size and porosity of the material.

3.3. Electrochemical impedance spectroscopy characterisation of G and NG derivatives

Electrochemical impedance spectroscopy (EIS) is a powerful technique which enables the evaluation of physical and interfacial

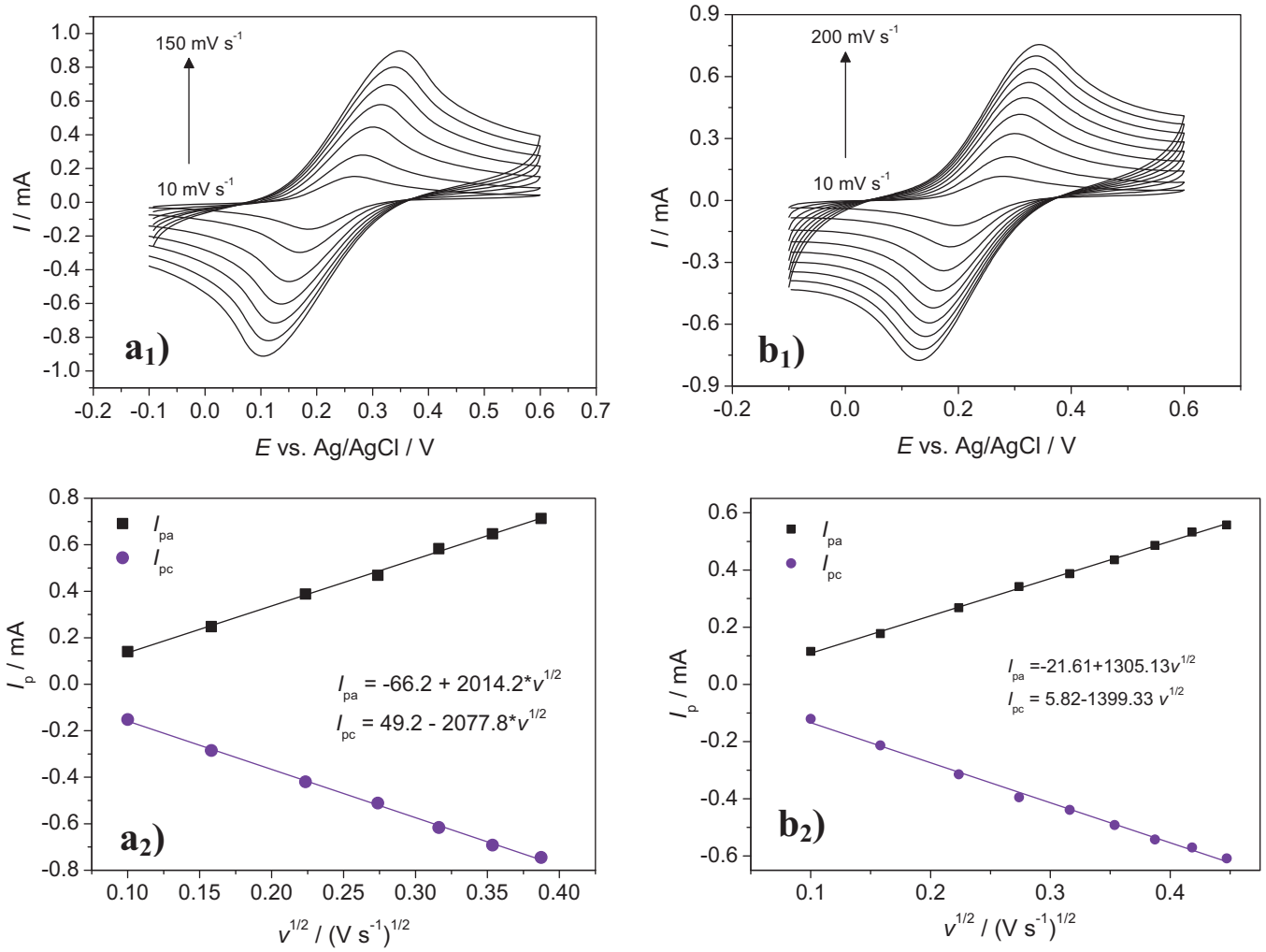

Fig. 2. Cyclic voltammograms recorded in 0.1 M KCl containing 3 mM $K_4[Fe(CN)_6]$ at different scan rates at (a_1) NG and (b_1) HNO_3_G modified GCE and in (a_2), (b_2) corresponding plots of I vs. $v^{1/2}$.

properties of modified electrodes. The technique was used to characterise NG, HNO_3_G, KOH_G and KOH_NG for which spectra were recorded in 0.1 M KCl at 0.0 V vs. Ag/AgCl, (close to the open circuit potential of all electrodes) and at 0.2 V vs. Ag/AgCl in 0.1 M KCl containing 3 mM $K_4[Fe(CN)_6]$ (close to the midpoint potential of Fe^{III}/Fe^{II}) and are shown in the complex plane plots in Fig. 4a and b. Fig. 4c shows spectra at the NG polymer composites, NG/PEDOT, PEDOT/NG, NG/PNR and PNR/NG, recorded in 0.1 M KCl at 0.0 V vs. Ag/AgCl.

As seen in Fig. 4a, in the case of GCE/HNO_3_G and GCE/KOH_NG in 0.1 M KCl, spectra have a high frequency semicircle, with larger diameter for HNO_3_G, while at NG and KOH_G, the spectra show close to 45° diffusive lines in the high frequency region. In the low frequency region, spectra recorded at all electrodes are characterised by capacitive lines, specific to graphene materials. This is indicative of restricted (finite) diffusion within the graphene layer. In the presence of redox probe, Fig. 4b, the impedance values decrease by one order of magnitude, beginning with semicircle for NG and HNO_3_G and all ending with diffusive lines.

The impedance spectra were fitted by using the equivalent circuit presented in Fig. 4d, sometimes without all the circuit elements. In the circuit, R_Ω is the cell resistance, R_{ct} represents the charge transfer at the solid–liquid interface, Z_W is the diffusional Warburg Element, CPE_{dl} and CPE_{pol} are constant phase elements representing the charge separation of the double layer and the polarisation of the graphene material, respectively. $CPE = [(Ci\omega)^\alpha]^{-1}$, modelled as a non-ideal capacitor, due to the porosity and non-homogeneity of the surface, with $0.5 < \alpha < 1$. The Warburg element, resulting from the equation $Z_W = R_D \text{cth}[(\tau i\omega)^\alpha] \times (\tau i\omega)^{-\alpha}$, where $\alpha < 0.5$, is characterised by a diffusional time constant (τ), a diffusional pseudocapacitance (C_D) and a diffusion resistance ($R_D = \tau/C_D$) [31]. It was not possible to model the spectra at low frequency using only finite diffusion, (i.e. without an extra capacitance), without significant errors.

Table 1
Ratio of electroactive area, A_{ele}, to geometric area, A_{geom}, of acid-treated graphite and different graphene modified electrodes and k_0 values calculated from cyclic voltammograms recorded at different scan rates in 3 mM $K_4[Fe(CN)_6]$ in 0.1 M KCl.

	GCE	HNO_3_Gr	G	NG	HNO_3_G	KOH_G	KOH_NG
A_{ele}/A_{geom}	0.59	1.90	0.60	4.30	2.80	2.80	2.90
$k_0 \times 10^4$ cm^{-1} s^{-1}	2.41	4.6	2.80	4.92	6.89	5.12	6.91

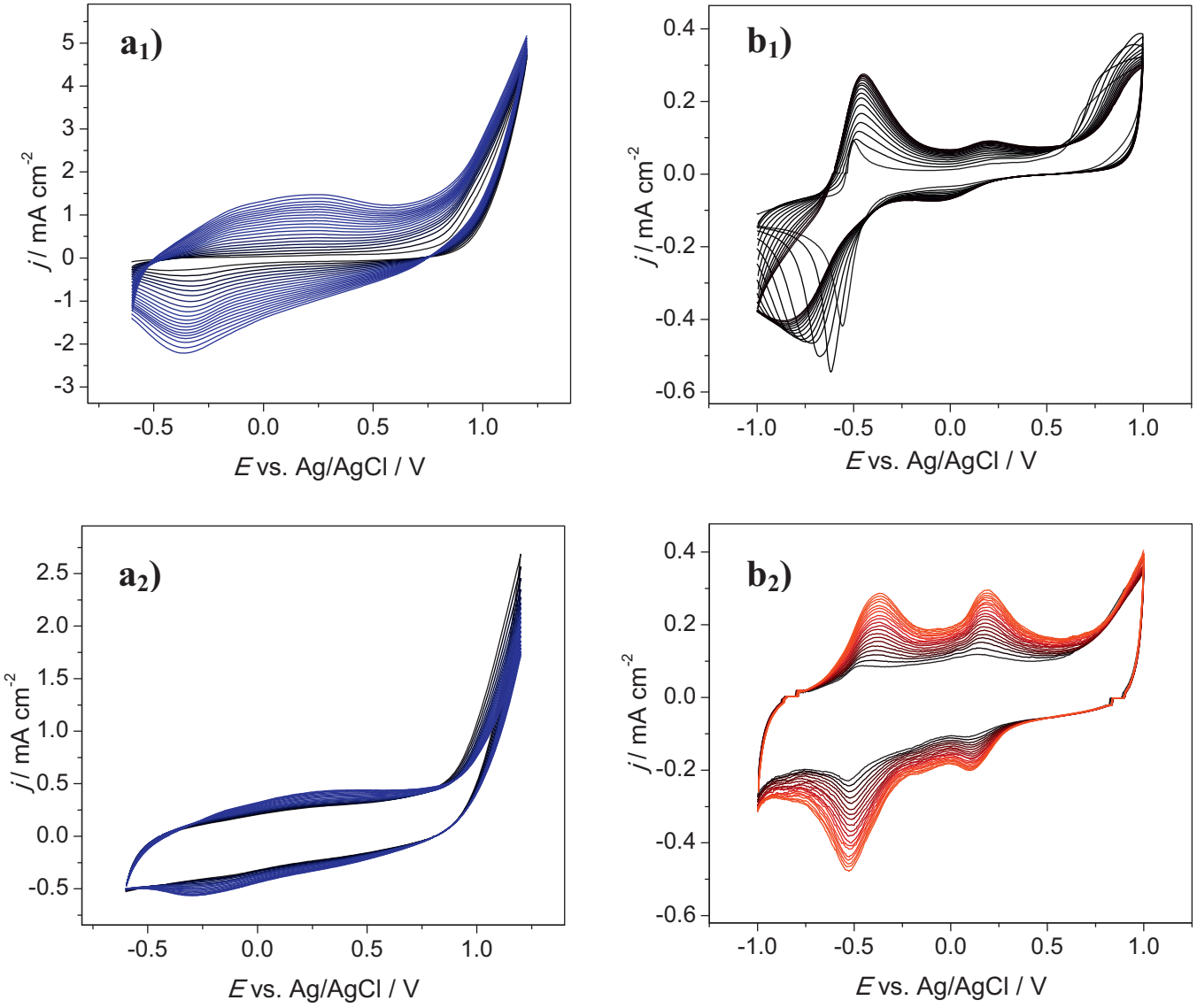

Fig. 3. Polymerisation of (a) EDOT from 10 mM EDOT in 0.1 M NaPSS and (b) NR from 1 mM NR in 0.025 M KPBS + 0.1 M KNO_3 on (a_1), (b_1) bare GCE and (a_2), (b_2) on GCE/NG.

Table 2 presents the values of the equivalent circuit elements from fitting of the spectra for NG, HNO_3_G, KOH_G and KOH_NG modified GCE. The fact that GCE/KOH_G presented a smaller Z_W value of 66.6 Ω cm^2 s$^{\alpha-1}$ and the highest CPE of 7.6 mF cm^{-2} s$^{\alpha-1}$ compared with 178.2 and 0.74, respectively, at HNO_3_G, demonstrates that functionalisation of the graphene in alkaline media leads to a more conductive material. For NG, the KOH functionalisation did not further improve its electrical conductivity, as suggested

Table 2
Resistance (R_{ct}), constant phase elements (CPE_{dl}, CPE_{pol}) and diffusional resistance and capacitance values obtained by equivalent circuit fitting of the impedance spectra from Fig. 4.

GCE modifier	R_{ct} (Ω cm^2)	CPE_{dl} (μF cm^{-2} s$^{\alpha-1}$)	α_1	Z_W (Ω cm^2 s$^{\alpha-1}$)	τ(s)	C_D (mF cm^{-2})	CPE_{pol}(mF cm^{-2} s$^{\alpha-1}$)	α_2
0.1 M KCl								
NG	–	–	–	263.3	3.7	14.1	2.30	0.90
HNO_3_G	109.5	56.2	0.83	178.2	1.0	5.6	0.74	0.60
KOH_G	–	–	–	66.6	0.6	9.0	7.61	0.83
KOH_NG	12.9	223.6	0.62	–	–	–	2.10	0.91
NG/PEDOT	108.2	143.5	0.76	–	–	–	1.70	0.77
PEDOT/NG	–	–	–	–	–	–	6.75	0.68
NG/NR	–	–	–	40.9	0.2	4.9	5.22	0.83
NR/NG	43.5	0.48	0.55	–	–	–	1.84	0.84
3 mM $K_4[Fe(CN)_6]$/0.1 M KCl								
NG	12.7	122.1	0.64	78.3	7.80	99.6	–	–
HNO_3_G	27.1	14.6	0.94	40.6	0.71	17.2	–	–
KOH_G	–	–	–	9.6	0.10	10.4	–	–
KOH_NG	–	–	–	6.2	0.06	9.6	–	–

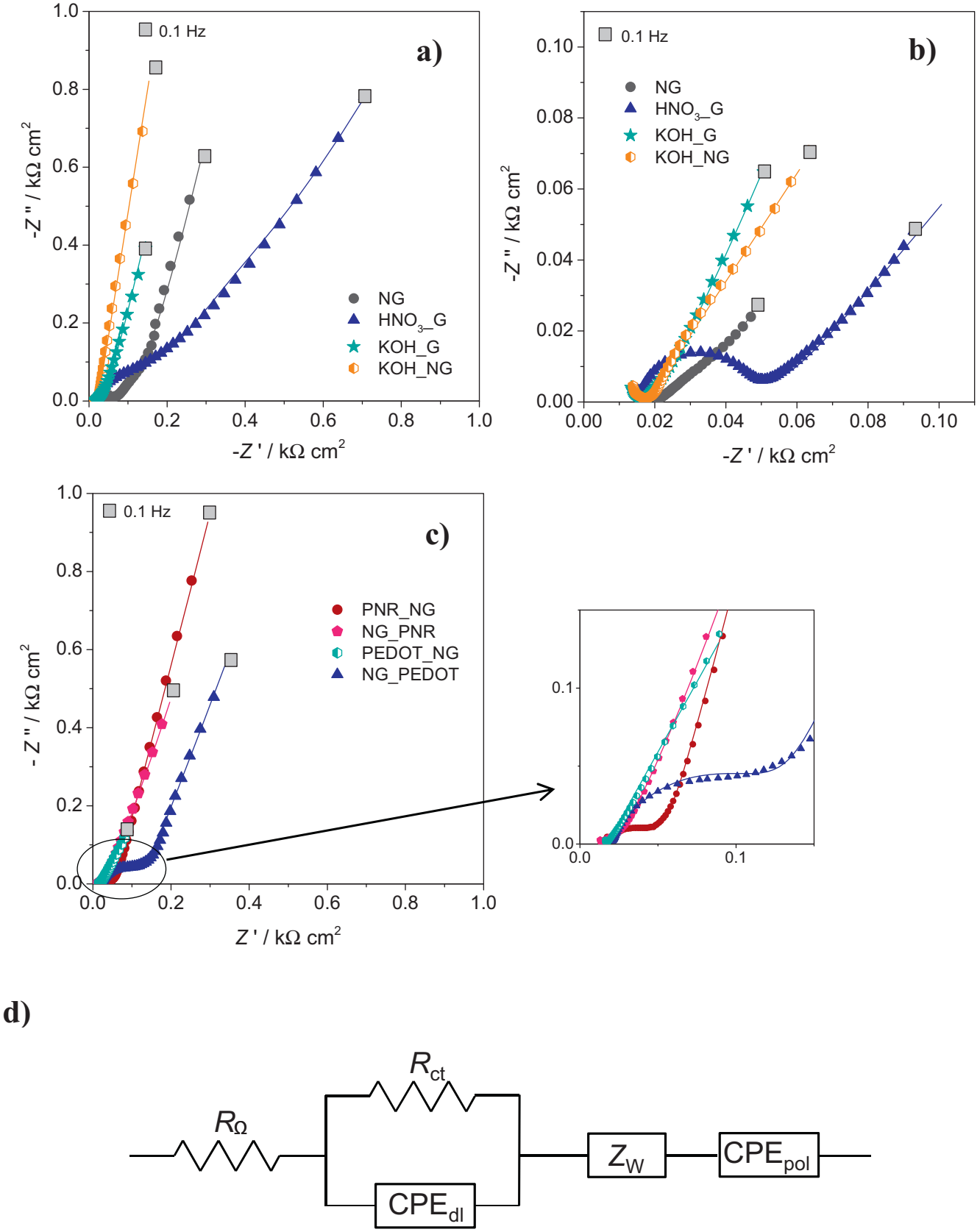

Fig. 4. Complex plane impedance plots recorded in (a) 0.1 M KCl and (b) 0.1 M KCl + 3 mM $K_4[Fe(CN)_6]$ for the GCE modified with NG, HNO_3_G, KOH_G and KOH_NG and (c) in 0.1 M KCl at GCE modified with NG/PEDOT; PEDOT/NG, NG/PNR and PNR/NG; the lines represent equivalent circuit fitting. (d) Equivalent circuits used to fit impedance spectra.

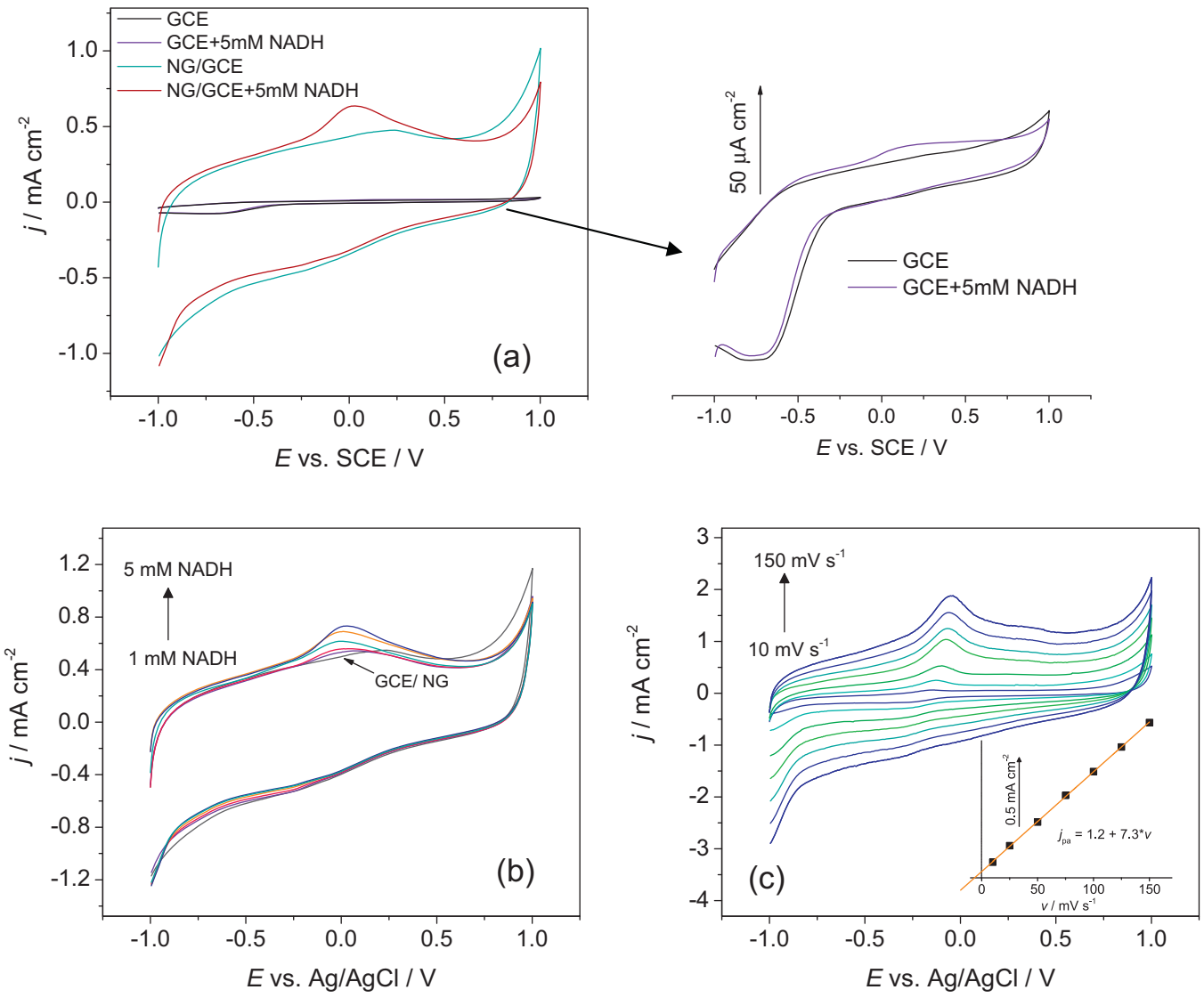

Fig. 5. (a) CVs at (a) GCE and GCE/NG in the presence of 5.0 mM NADH ($\upsilon = 50\,mV\,s^{-1}$); (b) at GCE/NG for different concentrations of NADH ($\upsilon = 50\,mV\,s^{-1}$); (c) at GCE/NG for different scan rates; supporting electrolyte 0.1 M NaPBS pH 7.0.

by very similar CPE_{pol} values, and as already expected from the CV data, since NG had a much higher electroactive area compared to KOH_NG.

In the presence of redox species, KOH_G/NG presented the lowest Z_W values of 9.6 and 6.2 $\Omega\,cm^2\,s^{\alpha-1}$, respectively, compared with 78.3 and 40.6 $\Omega\,cm^2\,s^{\alpha-1}$ for NG and HNO_3_G, suggesting that redox probe diffusion through KOH functionalised G and NG is facilitated. However, comparing the C_D values, it is observed that NG has a higher electronic conductivity, exhibiting a C_D of 99.6 $mF\,cm^{-2}$, far superior to that of the others: 17.2, 10.4 and 9.6 $mF\,cm^{-2}$ for HNO_3_G, KOH_G and KOH_NG, respectively. The charge transfer resistance was a factor of two lower, 12.7 $\Omega\,cm^2$ and the CPE value almost 10 times higher, 122.1 $\mu F\,cm^{-2}\,s^{\alpha-1}$ for NG than HNO_3_G, suggesting that NG is more appropriate for sensor applications.

EIS measurements were also performed at the redox polymer composites NG/PNR and PNR/NG modified GCE and conductive polymer composites NG/PEDOT, PEDOT/NG modified GCE.

Comparing the values of CPE_{dl}, CPE_{pol} and pseudocapacitance C_D from Table 2, it can be concluded that when PNR is polymerised on top of NG (NG/PNR), a composite with better conducting properties is formed, than PNR covered by NG (PNR/NG). This supports the CV data recorded during the polymerisation of the monomer on top of NG, (Fig. 3b_2).

On the contrary, in the case of the conducting polymer PEDOT, the composite containing NG on top of PEDOT shows better conducting properties than the inverse. The spectrum recorded at NG/PEDOT has a large diameter semicircle, with R_{ct} of 108.2 $\Omega\,cm^2$ and CPE_{dl} of 143.5 $mF\,cm^{-2}\,s^{\alpha-1}$, followed by a capacitive line, with CPE_{pol} 1.7 $mF\,cm^{-2}\,s^{\alpha-1}$, while PEDOT/NG exhibited only a capacitive line, with CPE_{pol} 6.8 $mF\,cm^{-2}$ $s^{\alpha-1}$, indicating that GCE/PEDOT/NG has superior conductivity than GCE/NG/PEDOT, in agreement with CV data (Fig. 3a).

To conclude, comparing all tested NG based polymer composites, from cyclic voltammetric and impedance spectroscopy studies, GCE/PEDOT/NG proved to be the best for sensor application in terms of higher electroactive area, better electron transfer rates and impedance parameters. Among all the modified electrodes tested, GCE/NG showed excellent electrochemical characteristics compared with acidic/basic functionalised G or NG as well as with conducting polymer/redox polymer composites of G or NG. Hence, further application studies were conducted using GCE/NG modified electrodes. However, we have demonstrated the various

plausible ways for functionalizing graphene or N-graphene and the promising enhancement in the electrochemical characteristics of graphene can be clearly seen. Thus acidic/basic functionalisation can be applied as easy alternative protocols for enhancing the properties of graphene and can find specific application in various fields such as supercapacitors [22].

3.4. Electrocatalytic applications of N-doped graphene to NADH and FAD

The fact that GCE/NG without any functionalisation exhibited the highest electroactive area and excellent electron transfer rates, prompted us to study the electrocatalytic ability of NG for the detection of important cofactors present in oxidase and dehydrogenase based enzymes, β-nicotinamide adenine dinucleotide (NADH) and flavin adenine dinucleotide (FAD).

Electro-oxidation of the cofactor NADH is of great interest as it is required for the whole library of dehydrogenase-based biosensors [32]. Direct electrooxidation of NADH to its corresponding oxidised form NAD^+ at bare/unmodified electrodes requires high activation energy, and proceeds with coupled reactions resulting in electrode fouling [33]. Hence an "ideal" NAD^+ probe should be capable of drastically reducing the oxidation potentials near to the formal redox potential of NAD^+/NADH i.e. −0.560 vs SCE [34] as well as enhancing the electron transfer rate. Electrochemical detection methods for NADH with high sensitivities have been reported, the major drawback being the high overpotential required at most electrodes, resulting in denaturation and subsequent poor stability of the enzymes [35]. Hence we have tested the electrocatalytic oxidation of NADH at NG modified GCE. CVs were recorded in 0.1 M NaPBS pH 7.0 at bare GCE and GCE/NG modified electrode in the presence of 5 mM NADH (see Fig. 5a) and for concentrations ranging from 1.0 to 5.0 mM NADH (see Fig. 5b). As observed from Fig. 5a, at GCE/NG the electrocatalytic oxidation of NADH occurs at −0.05 V, much closer to 0.0 V than the higher potential of ~0.25 V at bare GCE. A comparison of the present GC/NG modified electrode with previously reported ones [33] reveals that such high electrocatalytic effect is rarely observed for NADH oxidation. Only a few modified electrodes mentioned in [33], all containing 2 or 3 components, were able to oxidise NADH at potentials close to 0.0 V, e.g. carbon nanofibre/GCE, Meldola's blue based electrodes, toluidine blue/CNTs, 5,5′-dihydroxy-4,4′-bitryptamine/CNTs/Nafion/GCE, sol–gel silicate network/gold nanoparticles, among the 18 NADH sensors reported. This confirms the excellent electrocatalytic effect of GCE/NG on NADH oxidation, which will facilitate the functioning of dehydrogenase based enzymes at low potentials, therefore minimizing the influence of easily oxidisable interferents. Moreover, the NADH oxidation peak at GCE/NG, which increases linearly with the NADH concentration, see Fig. 5b, was much better defined and sharper, 50 times higher than the almost-flat low intensity peak at bare GCE, indicating a faster charge transfer process. Fig. 5c shows CVs at GCE/NG in the presence of 3 mM NADH at various scan rates. The linear dependence of current vs. scan rate confirms adsorption-controlled oxidation of NADH.

Another important cofactor present in many oxidoreductase enzymes is the flavoprotein coenzyme flavin adenine dinucleotide (FAD), which plays an important role in biochemical reactions [36]. Gorton and Johansson [37] had previously reported sluggish electron transfer and peak broadening of FAD at bare GCE (ΔE = 450 mV at 100 mV s^{-1}) resulting in lower peak currents due to a smaller surface coverage. Thus, electrocatalytic direct electron transfer is desirable for FAD, since mediator-assisted electron shuttling is usually employed in FAD dependent oxidases. Moreover, for future application, FAD is needed in biofuel cells based on genetically engineered FAD based enzyme, which are being developed to improve the stability of biofuel cells for long-term operation

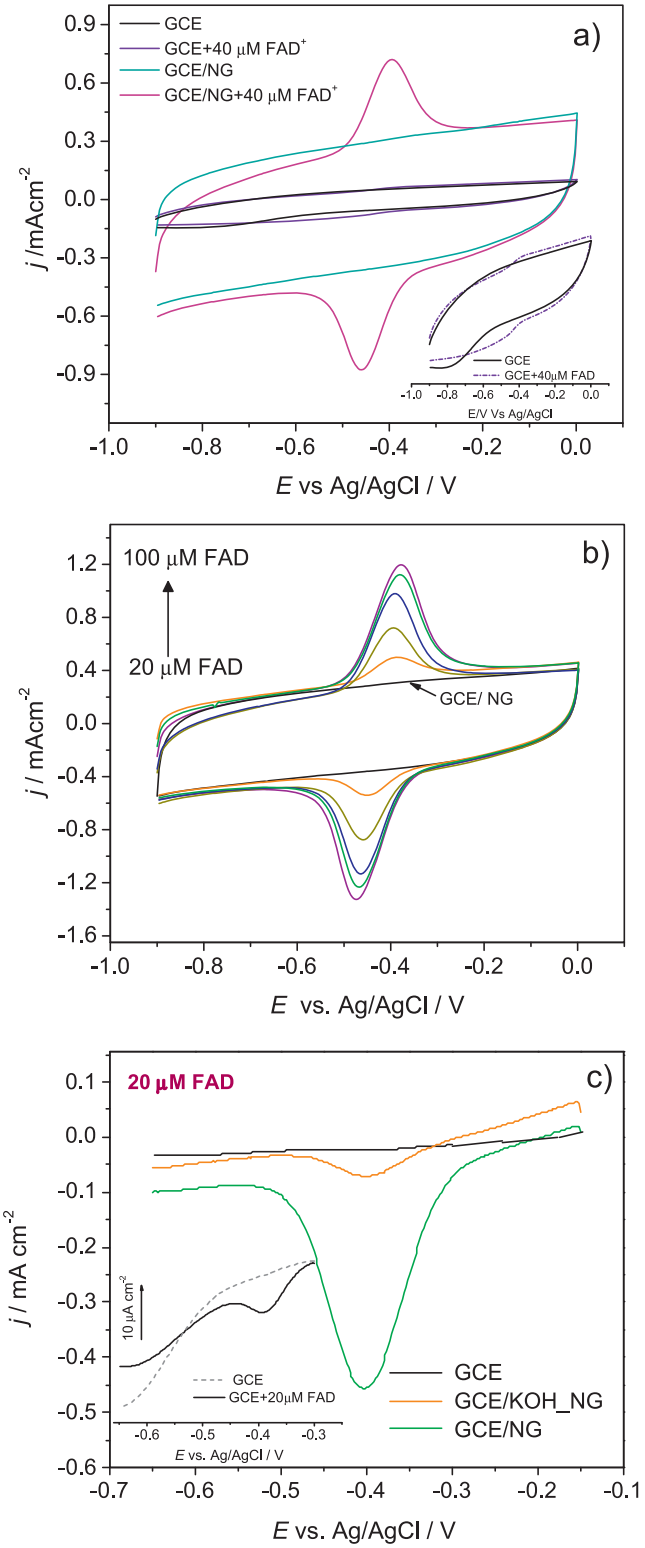

Fig. 6. (a) CVs at GCE and GCE/NG in the presence of 40 μM FAD and (b) CVs at GCE/NG for different concentrations of FAD at ν = 50 mV s^{-1} and (c) DPVs in the presence of 20 μM FAD at 10 mV s^{-1} (amplitude 25 mV); supporting electrolyte 0.1 M NaPBS pH 7.0.

[38], Fig. 6a shows cyclic voltammograms of 40 μM FAD at bare and NG modified GCEs in 0.1 M NaPBS pH 7.0. As observed, FAD peaks can hardly be seen at GCE, with a quasi-reversible behaviour (ΔE = 180 mV) while at GCE/NG the peaks are very well defined, with a small peak-to-peak separation (ΔE = 63 mV). Additionally,

highly enhanced anodic (~40 fold) and cathodic (~16 fold) peak currents of FAD were observed at GCE/NG compared with bare GCE. The oxidation and reduction peaks are at −0.40 V and −0.46 V vs. Ag/AgCl (E_m = 0.43 V)

The cathodic and anodic peak currents of the CVs recorded at scan rates from 10 to 300 mV s^{-1}, were linearly dependent with the scan rates, with the linear regressions $j_{pa} = 0.4 + 107.0c$ and $j_{pa} = 0.4 + 122.9c$, meaning that the redox process is adsorption controlled. Fig. 6b shows cyclic voltammograms for increasing concentrations of FAD from 20 to 100 μM at the GCE/NG, with a linear range only up to 60 μM, probably because of FAD adsorption. Since the FAD/$FADH_2$ redox couple showed excellent redox behaviour on GCE/NG, its electrochemical behaviour was also tested at GCE/KOH_NG. Fig. 6c shows DPV curves in the presence of 20 μM FAD at bare GCE, NG and KOH_NG modified GCE and the peak current was 50 and 7 times higher at NG and KOH_NG modified GCE, respectively, compared to bare GCE. These observations clearly indicate the advantageous effect of nitrogen doping in enhancing the electrochemical properties of graphene.

The FAD/$FADH_2$ redox couple is widely used as a mediator for NAD^+ regeneration, which is critical for the functioning of dehydrogenase enzyme based biosensors. The easiest way to achieve NAD^+ regeneration is traditionally carried out by redox mediators [33]. Here, we have shown the direct oxidation of NADH at GCE/NG modified electrode. In addition, the better reversibility and enhanced current densities observed in the case of the FAD/$FADH_2$ system obviously paves the way for use as redox mediators of NAD^+ regeneration. The enhanced electrochemical characteristics of the FAD/$FADH_2$ system at GC/NG also illustrate its applicability as a suitable substrate for FAD based enzyme biosensors such as glucose oxidase or xanthine oxidase. Such applications will be pursued in future studies.

4. Conclusions

In the present work, we have developed various modified electrodes with graphene and nitrogen doped graphene, its acidic/basic derivatives and polymer composites and thorough electrochemical characterisation of the modified electrodes has been conducted. The HNO_3_G and KOH_G/NG modified GCE increased the GCE electroactive area by a factor of almost 3, the k_0 values also being increased from 2.4 for GCE to 5.2 and 6.9×10^{-4} cm s^{-1} for HNO_3_G and KOH_G/NG modified GCE. In the case of composite material it was observed that when PNR is polymerised on top of NG (NG/PNR), the composite formed has better conducting properties, than PNR/NG, while in the case of PEDOT, the composite containing NG on top of PEDOT (PEDOT/NG) showed itself to be superior. The application potential of these electrodes in the electrocatalysis of enzyme cofactors has been successful demonstrated. Among the various modified electrodes, the N-graphene modified GCE has shown higher sensitivities than the other electrodes. This proves that heteroatom N-doped graphene is far superior to graphene or its derivatives/polymer composites, due to its n-type semiconductor like properties, making N-doped graphene a ready-to-use electrode material.

Acknowledgements

Financial support from Fundação para a Ciência e a Tecnologia (FCT), Portugal PTDC/QUI-QUI/116091/2009, POCH, POFC-QREN (co-financed by FSE and European Community FEDER funds through the program COMPETE and FCT project PEst-C/EME/UI0285/2013) is gratefully acknowledged. K.P.P. and M.M.B. thank FCT for postdoctoral fellowships SFRH/BPD/78939/2011 and SFRH/BPD/72656/2010. The research from Canada was supported by Natural Sciences and Engineering Research Council of Canada (NSERC) and Canada Research Chair (CRC) Program.

References

[1] J. Wang, Electrochemical glucose biosensors, Chem. Rev. 108 (2008) 814–825.
[2] C. Chen, Q. Xie, D. Yang, H. Xiao, Y. Fu, Y. Tan, S. Yao, Recent advances in electrochemical glucose biosensors: a review, RSC Adv. 3 (2013) 4473–4491.
[3] Z. Zhu, L. Garcia-Gancedo, A.J. Flewitt, H. Xie, F. Moussy, W.I. Milne, A critical review of glucose biosensors based on carbon nanomaterials: carbon nanotubes and graphene, Sensors 12 (2012) 5996–6022.
[4] B. Willner, I. Willner, Reconstituted redox enzymes on electrodes: from fundamental understanding of electron transfer at functionalized electrode interfaces to biosensor and biofuel cell applications, in: I. Willner, E. Katz (Eds.), Bioelectronics: From Theory to Applications, WileyVCH, Weinheim, 2005, p. 35.
[5] M.V. Pishko, I. Katakis, S.E. Lindquist, L. Ye, B.A. Gregg, A. Heller, Direct electrical communication between graphite electrodes and surface adsorbed glucose oxidase/redox polymer complexes, Angew. Chem. Int. Ed. 29 (1990) 82–84.
[6] I. Willner, E. Katz, B. Willner, Electrical contact of redox enzyme layers associated with electrodes: routes to amperometric biosensors, Electroanalysis 9 (1997) 965–977.
[7] A. Bianco, K. Kostarelos, M. Prato, Opportunities and challenges of carbon-based nanomaterials for cancer therapy, Expert Opin. Drug Deliv. 5 (2008) 331–342.
[8] L. Rodríguez-Pérez, M.A. Herranza, N. Martín, The chemistry of pristine graphene, Chem. Commun. 49 (2013) 3721–3735.
[9] I.V. Lightcap, P.V. Kamat, Graphitic design: prospects of graphene-based nanocomposites for solar energy conversion, storage, and sensing, Acc. Chem. Res. 46 (2013) 2235–2243.
[10] D. Usachov, O. Vilkov, A. Grüneis, D. Haberer, A. Fedorov, V.K. Adamchuk, A.B. Preobrajenski, P. Dudin, A. Barinov, M. Oehzelt, C. Laubschat, D.V. Vyalikh, Nitrogen-doped graphene: efficient growth, structure, and electronic properties, Nano Lett. 11 (2011) 5401–5417.
[11] R. Lv, M. Terrones, Towards new graphene materials: doped graphene sheets and nanoribbons, Mater. Lett. 78 (2012) 209–218.
[12] H. Liu, Y. Liu, D. Zhu, Chemical doping of graphene, J. Mater. Chem. 21 (2011) 3335–3345.
[13] Y. Xin, J. Liu, X. Jie, W. Liu, F. Liu, Y. Yin, J. Gu, Z. Zou, Preparation and electrochemical characterisation of nitrogen doped graphene by microwave as supporting materials for fuel cell catalysts, Electrochim. Acta 60 (2012) 354–358.
[14] G. Yang, Z. Kang, X. Ye, T. Wu, Q. Zhu, Molecular simulation of flavin adenine dinucleotide immobilized on charged single-walled carbon nanotubes for biosensor applications, Biomaterials 33 (2012) 8757–8770.
[15] C. Deng, J. Chen, X.C. Chen, X.L. Nie, S. Yao, Direct electrochemistry of glucose oxidase and biosensing for glucose based on boron-doped carbon nanotubes modified electrode, Biosens. Bioelectron. 23 (2008) 1272–1277.
[16] W. Yang, K.R. Ratinac, S.P. Ringer, P. Thordarson, J.J. Gooding, F. Braet, Carbon nanomaterials in biosensors: should you use nanotubes or graphene? Angew. Chem. Int. Ed. 49 (2010) 2114–2338.
[17] X. Dai, G.G. Wildgoose, R.G. Compton, Apparent 'electrocatalytic' activity of multiwalled carbon nanotubes in the detection of the anaesthetic halothane: occluded copper nanoparticles, Analyst 31 (2006) 901–916.
[18] L. Zhao, R. He, K.T. Rim, T. Schiros, K.S. Kim, H. Zhou, C. Gutiérrez, S.P. Chockalingam, C.J. Arguello, L. Palova, D. Nordlund, M.S. Hybertsen, D.R. Reichman, T.F. Heinz, P. Kim, A. Pinczuk, G.W. Flyn, A.M. Pasupathy, Visualizing individual nitrogen dopants in monolayer graphene, Science 133 (2011) 998–1003.
[19] T. Schiros, D. Nordlund, L. Pálová, D. Prezzi, L. Zhao, K.S. Kim, U. Wurstbauer, C. Gutiérrez, D. Delongchamp, C. Jaye, D. Fischer, H. Ogasawara, L.G.M. Pettersson, D.R. Reichman, P. Kim, M.S. Hybertsen, A.N. Pasupathy, Connecting dopant bond type with electronic structure in n-doped graphene, Nano Lett. 12 (2012) 4025–4031.
[20] Y. Wang, Y. Shao, D.W. Matson, J.L. Li, Y. Lin, Nitrogen-doped graphene and its application in electrochemical biosensing, ACS Nano 4 (2010) 1790–1798.
[21] V. Georgakilas, M. Otyepka, A.B. Bourlinos, V. Chandra, N. Kim, K.C. Kemp, P. Hobza, R. Zboril, K.S. Kim, Functionalisation of graphene: covalent and non-covalent approaches, derivatives and applications, Chem. Rev. 112 (2012) 6156–6214.
[22] Y. Zhu, S. Murali, M.D. Stoller, K.J. Ganesh, W. Cai, P.J. Ferreira, A. Pirkle, R.M. Wallace, K.A. Cychosz, M. Thommes, D. Su, E.A. Stach, R.S. Ruoff, Carbon-based supercapacitors produced by activation of graphene, Science 332 (2011) 1537–1541.
[23] D. Geng, S. Yang, Y. Zhang, J. Yang, J. Liu, R. Li, T. Sham, X. Sun, S. Ye, S. Knights, Nitrogen doping effects on the structure of graphene, Appl. Surf. Sci. 257 (2011) 9193–9198.
[24] C.M.A. Brett, A.M. Oliveira-Brett, Electrochemistry, Principles, Methods and Applications, Oxford University Press, Oxford, 1993, pp. 174–185, Chapter 9.
[25] K. Wang, J. Lu, L. Zuang, Direct determination of diffusion coefficient for borohydride anions in alkaline solutions using chronoamperometry with spherical Au electrodes, J. Electroanal. Chem. 585 (2005) 191–196.
[26] R.J. Rice, N.M. Pontikos, R.L. McCreery, Quantitative correlations of heterogeneous electron-transfer kinetics with surface properties of glassy carbon electrodes, J. Am. Chem. Soc. 112 (1990) 4617–4622.

[27] S. Kakhki, M.M. Barsan, E. Shams, C.M.A. Brett, New robust redox and conducting polymer modified electrodes for ascorbate sensing and glucose biosensing, Synth. Met. 161 (2012) 2718–2726.
[28] M.M. Barsan, E.M. Pinto, M. Florescu, C.M.A. Brett, Development and characterisation of a new conducting carbon composite electrode, Anal. Chim. Acta 635 (2009) 71–78.
[29] M.E. Ghica, C.M.A. Brett, The influence of carbon nanotubes and polyazine redox mediators on the performance of amperometric enzyme biosensors, Microchim. Acta 170 (2010) 257–265.
[30] R.C. Carvalho, C. Gouveia-Caridade, C.M.A. Brett, Glassy carbon electrodes modified by multiwalled carbon nanotubes and poly(neutral red): a comparative study of different brands and application to electrocatalytic ascorbate determination, Anal. Bioanal. Chem. 398 (2010) 1675–1685.
[31] E. Barsoukov, in: J.R. Macdonald (Ed.), Impedance Spectroscopy Theory Experiment Applications, second ed., Wiley, New York, 2005.
[32] K.S. Prasad, J.C. Chen, C. Ay, J.M. Zen, Mediatorless catalytic oxidation of NADH at a disposable electrochemical sensor, Sens. Actuators, B—Chem. 123 (2007) 715–729.
[33] A. Radoi, D. Compagnone, Recent advances in NADH electrochemical sensing design, Bioelectrochemistry 76 (2009) 126–134.
[34] W.M. Clark, Oxidation–Reduction Potentials of Organic System, R.E. Krieger Publishing, Huntington, NY, 1972.
[35] M. Pumera, R. Scipioni, H. Iwai, T. Ohno, Y. Miyahara, M. Boero, A mechanism of adsorption of *b*-nicotinamide adenine dinucleotide on graphene sheets: experiment and theory, Chem. Eur. J. 15 (2009) 10851–10856.
[36] S. Hustad, P.M. Ueland, J. Schneede, Quantification of riboflavin, flavin mononucleotide, and flavin adenine dinucleotide in human plasma by capillary electrophoresis and laser-induced fluorescence detection, Clin. Chem. 45 (1999) 862–868.
[37] L. Gorton, G. Johansson, Cyclic voltammetry of FAD adsorbed on graphite, glassy carbon, platinum and gold electrodes, J. Electroanal. Chem. 113 (1980) 151–158.
[38] Z. Zhu, C. Momeu, M. Zakhartsev, U. Schwaneberg, Making glucose oxidase fit for biofuel cell applications by directed protein evolution, Biosens. Bioelectron. 21 (2006) 2046–2051.